第31卷第5期
2012年10月

红外与毫米波学报
J. Infrared Millim. Waves

Vol. 31, No. 5
October, 2012

文章编号:1001 - 9014(2012)05 - 0385 - 05

DOI:10.3724/SP. J. 1010. 2012. 00385

Properties of lattice matched quaternary InAlGaAs on InP substrate grown by gas source MBE

WANG Kai[1,2], GU Yi[1,3], FANG Xiang[1,2], ZHOU Li[1,2],
LI Cheng[1,2], LI Hao-Si-Bai-Yin[1], ZHANG Yong-Gang[1,3]*

(1. State Key Laboratory of Functional Materials for Informatics, Shanghai Institute of Microsystem and Information Technology, Chinese Academy of Sciences, Shanghai 200050, China;
2. Graduate School of the Chinese Academy of Sciences, Beijing 100049, China;
3. Key Laboratory of Infrared Imaging Materials and Detectors, Chinese Academy of Science, Shanghai 200083, China)

Abstract: Properties of quaternary InAlGaAs alloys prepared by gas source MBE growth have been investigated with high resolution X-ray diffraction rocking curves, photoluminescence and Hall measurements. X-ray rocking curves show that all the samples are well matched to InP substrate according to calibration data. The photoluminescence and Hall measurement show that the PL intensity, electron concentration and mobility decrease distinctly as Al composition increases. The group III compositions are determined from both photoluminescence and x-ray diffraction measurements, and agreed well with the designed values. The relationship between the designed Al compositions and measured values provides us a practical way for the precise composition control.

Key words: compound semiconductor; molecular beam epitaxy; InAlGaAs; X-ray diffraction; photoluminescence
PACS: 81.05.Ea, 81.15.Hi, 61.05.cp

InP衬底上晶格匹配四元系InAlGaAs的气态源分子束外延生长

王 凯[1,2], 顾 溢[1,3], 方 祥[1,2], 周 立[1,2],
李 成[1,2], 李好斯白音[1], 张永刚[1,3]*

(1. 中国科学院上海微系统与信息技术研究所 信息功能材料国家重点实验室,上海 200050;
2. 中国科学院研究生院,北京 100049;
3. 中国科学院红外成像材料与器件重点实验室,上海 200083)

摘要:采用高分辨率X射线衍射摇摆曲线、光致发光以及霍尔测试对采用气态源分子束外延方法生长的四元系InAlGaAs材料性质进行了表征。摇摆曲线结果表明,根据计算数据所生长的InAlGaAs样品与InP衬底基本匹配.光致发光和霍尔测试结果显示随着Al组分的增加,样品的光致发光强度、电子浓度和迁移率均有所下降.样品的三族元素组分由光致发光及X射线衍射实验获得,测试结果与设计值吻合,Al组分的实验设计值与测试结果的关系提供了一种实用的精确控制组分的方法.

关 键 词:化合物半导体;分子束外延;InAlGaAs;X射线衍射;光致发光
中图分类号:TN2 **文献标识码**:A

Introduction

Quaternary alloy $In_xAl_yGa_zAs$ $(x + y + z = 1)$, which can be considered as a quasi-ternary alloy of three binaries InAs, AlAs and GaAs, has attracted much attention especially in optoelectronics[1-3]. The lattice of $In_xAl_yGa_zAs$ quaternary can be matched to InP when $x \approx 0.53$[4], which makes it an important

Received date: 2011 - 04 - 26, **revised date**: 2011 - 06 - 09 **收稿日期**:2011 - 04 - 26, **修回日期**:2011 - 06 - 09
Foundation items: Supported by National Basic Research Program of China (2012CB619202), Founding of Key Laboratory of Infrared Imaging Materials and Detectors, Chinese Academy of Sciences and Innovative Founding of Shanghai Institute of Microsystem and Information Technology, Chinese Academy of Sciences.
Biography: WANG Kai, (1984-), male, Shanghai, Ph. D. candidate. Research area is optoelectronic materials and devices.
* **Corresponding author**: E-mail: ygzhang@ mail. sim. ac. cn.

epitaxial material choice from both research and application points of view. It's well known that the performances of photodetectors and their focal plane arrays (FPAs) are related to the bandgap of the materials directly. Si detectors exhibit outstanding performance only at wavelengths below 1.1 μm. At longer wavelength up to about 1.7 μm $In_{0.53}Ga_{0.47}As$ with lattice matched to InP are among the first-rank. Nevertheless, in the wavelength range between 1.1 ~ 1.7 μm there exist many important applications which require better devices. For example, the cloud differentiation in remote sensing needs FPAs with peak performance around 1.3 ~ 1.4 μm. Also, the singlet oxygen detection in medical sensing needs more sensitive PDs peaking at 1.27 μm. However, in these applications the best performance could not be reached for the narrower bandgap $In_{0.53}Ga_{0.47}As$. In this case a lattice matched materials with adjustable wider bandgap should be preferable.

When lattice matched to InP, InAlGaAs [or $(In_{0.53}Ga_{0.47}As)_m(In_{0.52}Al_{0.48}As)_{1-m}$] can be regarded as the combination of two ternary alloys $In_{0.53}Ga_{0.47}As$ and $In_{0.52}Al_{0.48}As$, and its band-gap can be tailored between 0.74 eV ($In_{0.53}Ga_{0.47}As$) and 1.47 eV ($In_{0.52}Al_{0.48}As$) at room temperature. InAlGaAs has been employed in the demonstrations of electrical and optoelectronic devices, such as laser [3, 5-6], quantum well photodetector [2,6], heterojunction bipolar transistor[8-9] and high electron mobility transistor[10-11]. InAlGaAs is suitable to be grown using molecular beam epitaxy (MBE) because of the stable stick coefficients of the group III elements which provides reproducible mole fraction in the growth of alloys[12]. Furthermore, only one group V element is incorporated in this alloy, which avoids the problems of As-P ratio control. However, the precise control of the bandgap in lattice matched condition remains a challenge as the ratio of three group III elements needs to be redressed simultaneously. Meanwhile, the compositions of this quaternary alloy could not be determined using only X-ray diffraction measurement as those of ternaries. In this paper, the growth of quaternary InAlGaAs lattice matched to InP substrate was demonstrated using gas source MBE, the group III compositions of the samples were determined, their optical and electrical properties were investigated as well. A practical method to control the compositions of the alloy precisely was also discussed.

1 Experimental details

The samples were grown on (100)-oriented InP epi-ready substrates in a VG Semicon V80H gas source MBE system. The effusion cells containing In, Al and Ga were used as group III sources, their fluxes were controlled by changing the cell temperatures. Arsine (AsH_3) and phosphine (PH_3) cracking cells were used as group V sources, their fluxes were pressure controlled. Standard Si effusion cell was used as n-type doping source, and the doping levels were also controlled by changing the cell temperatures. Before the growth, the fluxes of group III sources were calibrated by using an in-situ ion gauge. All the grown samples were designed lattice matched to InP substrate. The designed In, Al and Ga compositions of $In_xAl_yGa_zAs$ were estimated using the flux values from the following equations:

$$x = \frac{a \cdot f_{In}}{a \cdot f_{In} + b \cdot f_{Al} + c \cdot f_{Ga}},$$

$$y = \frac{b \cdot f_{Al}}{a \cdot f_{In} + b \cdot f_{Al} + c \cdot f_{Ga}},$$

$$z = \frac{c \cdot f_{Ga}}{a \cdot f_{In} + b \cdot f_{Al} + c \cdot f_{Ga}}, \quad (1)$$

where f_{In}, f_{Al} and f_{Ga} are the fluxes of In, Al and Ga sources respectively; a, b and c are the weighting factors for In, Al and Ga, which are related to the position of effusion cells and the species of the sources.

At first, InP-lattice-matched $In_{0.53}Ga_{0.47}As$ and $In_{0.52}Al_{0.48}As$ calibration samples were grown, and the corresponding source fluxes were calibrated and the relative ratios of a, b and c were obtained. Then, InAlGaAs samples were grown with the calibrated flux data. The designed Al compositions of InAlGaAs sample 1, 2 and 3 were 0.216, 0.242 and 0.266 according to Equation (1) and calibrated flux data, respectively. The thicknesses of all the samples were around 0.5 μm, and the growth rates were about 1 μm/h. The lattice-matched InGaAs and InAlAs samples were denoted as sample 4 and 5 hereafter for reference. All the samples were doped with Si at the same cell temperature.

After growth, the (004) $\omega/2\theta$ rocking curves were measured using a Philips X'pert MRD HRXRD equipped with a four-crystal Ge (220) monochromator. The PL spectra at room temperature (RT) were measured using a Nicolet Megna 860 Fourier transform infrared (FTIR) spectrometer, in which CaF2

beam splitter and InGaAs or InSb detector were used. A 100 mW diode pumped solid-state (DPSS) laser (λ = 473 nm) was used as an excitation source. Hall measurements at RT were performed on an Accent HL5500 Hall system to determine the carrier concentration and mobility.

2 Results and discussions

All the samples show mirror-like surface morphology without haziness or cross-hatching under an optical microscope. Figure 1 shows the HRXRD (004) $\omega/2\theta$ rocking curves of different samples, and Table 1 lists the extracted results. Two main peaks can be observed for each rocking curve, where the left peak corresponds to InP substrate, and the right peak corresponds to epi-layer. The full widths at half-maximum (FWHM) for samples 1, 2 and 3 are 37.9 s, 53.6 s and 51.9 s respectively, which are approximate to those of $In_{0.53}Ga_{0.47}As$ and $In_{0.52}Al_{0.48}As$ samples, and comparable to the reported results of the solid source MBE (SSMBE) grown samples[12]. It is noticed that sample 2 has relatively larger FWHM for both substrate and epi-layer peaks, which is possibly due to the inferior substrate quality of this sample. As the lattice constants of AlAs and GaAs are very close (their mismatch is only 0.14% at 300 K), the In composition of each sample can be estimated from the average of the two In composition values when assuming the epi-layer is InGaAs or InAlAs, and so is the mismatch with InP. It can be seen that all the epi-layers have small negative lattice mismatches ($\Delta a/a < -6.1\times10^{-4}$) with InP substrate.

Table 1　Extracted results from HRXRD measurements
表 1　从 HRXRD 测试获得的结果

Samples	Material	Mismatch $\Delta a/a$/ppm	In composition	FWHM of epi-layer/arcsec
1	InAlGaAs	-605	0.517	37.9
2	InAlGaAs	-402	0.520	53.6
3	InAlGaAs	-266	0.522	51.9
4	InGaAs	-186	0.528	39.6
5	InAlAs	-249	0.518	55.1

All the grown InAlGaAs samples show moderate PL signals at room temperature. Figure 2 shows the results including that of sample 4 (InGaAs) as a reference. The PL signals of three InAlGaAs samples were measured using InGaAs detector, whereas the PL data of sample 4 was proportionally transformed from the signal measured using InSb detector. From

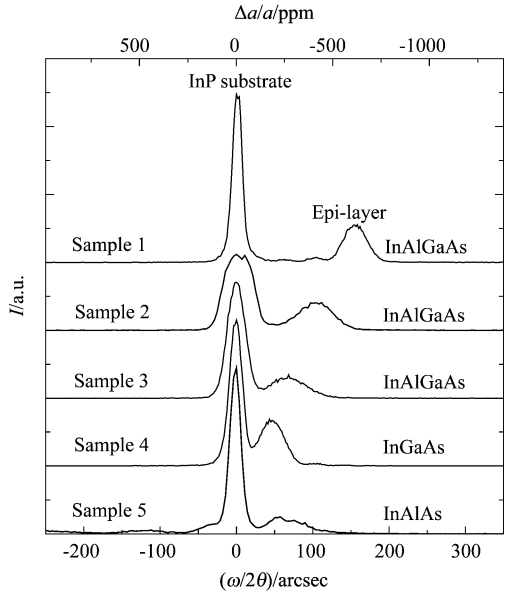

Fig. 1　HRXRD (004) $\omega/2\theta$ rocking curves of different samples
图 1　不同样品的 HRXRD (004) $\omega/2\theta$ 摇摆曲线

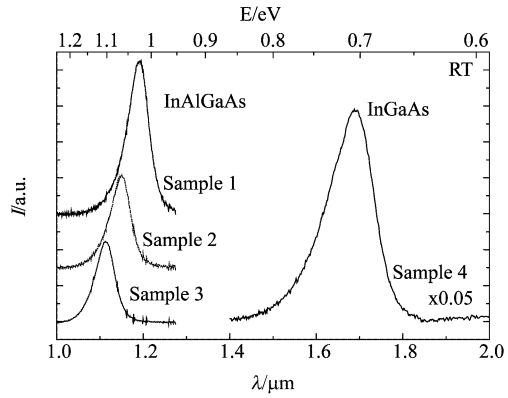

Fig . 2　PL spectra of different samples at room temperature
图 2　不同样品的室温 PL 光谱

Fig. 2, it can be seen that the PL intensity decreases distinctly with the increase of the Al composition, mainly due to the approach of Γ and X valley [1]. No PL signal is observed for sample 5 mainly due to the even lower PL efficiency of InAlAs at room temperature. The energy of PL peak for sample 4 is 0.734 eV, which is very close to the theoretical RT band-gap of lattice matched $In_{0.53}Ga_{0.47}As$ material. The energies of PL peaks for samples 1-3 are 1.04 eV, 1.08 eV and 1.11 eV, while the FWHM are 51.5 meV, 52.0 meV and 54.3 meV, respectively. Those FWHM are comparable to the results grown using SSMBE[12]. Assuming the band-gap is the same as

the measured PL energy and using the In composition extracted from HRXRD measurements, the Al compositions of samples 1-3 are determined to be 0.234, 0.259 and 0.283, respectively.

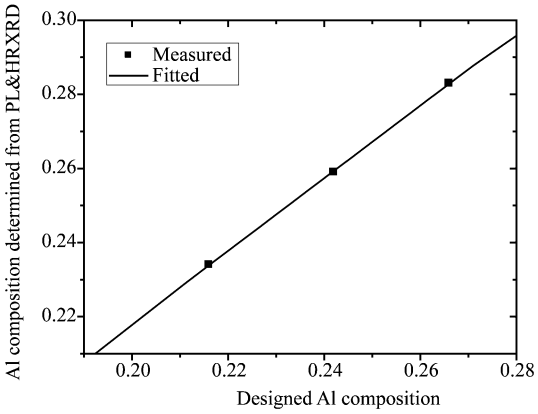

Fig . 3 The Al composition x extracted from HRXRD and PL measurements versus the designed Al composition
图3 由 HRXRD 和 PL 测试得到的 Al 组分值与设计值的关系图

Figure 3 shows the Al composition extracted from HRXRD and PL measurements as a function of the designed Al composition from equation (1). The solid line with a slope of about 0.98 is the fitted line from the measured points. It could be seen that the measured values are 0.017, 0.017 and 0.018 larger than the designed values, therefore the Al control precisions are 7.9%, 7.0% and 6.4% for samples 1, 2 and 3 respectively. The calibration results could be used for the growth of InAlGaAs samples with the known flux data.

The electrical properties of the samples were also investigated. Figure 4 shows the electron concentration and mobility at different Al compositions at room temperature. It can be seen that as the Al composition increases, both of the electron concentration and the mobility decrease significantly. This is mainly because Γ valley becomes more close to X valley when the Al content is increased[1], and there are more opportunities for electrons to occupy X valley. Since the mobility of the electrons in X valley is very low, the electron mobility decreases dramatically with the increase of Al content. For the pure InAlAs sample, the electron concentration value of 10^{14} cm^{-3} is somewhat uncertain, as the epi-layer is not thick enough to exceed the depletion region during the Hall measurement.

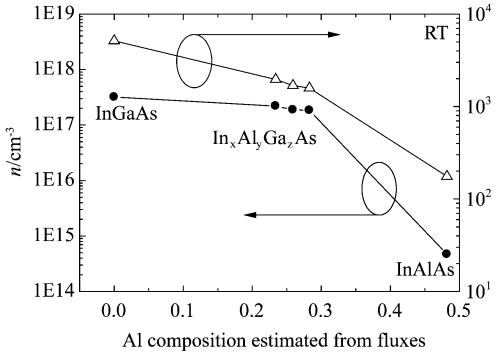

Fig . 4 The electron concentration and mobility of different samples at room temperature
图4 室温下不同样品的电子浓度和迁移率

3 Conclusions

In conclusion, the quaternary InAlGaAs samples with lattice matched to InP have been grown by gas source MBE and investigated in detail. The HRXRD (004) $\omega/2\theta$ rocking curves show that all the samples are well matched to InP substrates. The PL and Hall measurement show that the PL intensity, electron concentration and mobility decrease when Al compositions increase mainly because of the change of the band structure. The relationship between the designed Al composition and measured values from HRXRD and PL measurements provides us a practical way for precise composition control in quaternary InAlGaAs growth.

REFERENCES

[1] Vurgaftman I, Meyer J R, Ram-Mohan L R. Band parameters for III-V compound semiconductors and their alloys [J]. Journal of Applied Physics, 2001, **89**(11): 5815 - 5875.

[2] Jelen C, Slivken S, Guzman V ,et al. InGaAlAs-InP quantum-well infrared photodetectors for 8-20-μm wavelengths [J]. IEEE Journal of Quantum Electronics, 1998, **34**(10): 1873 - 1876.

[3] Chang H L, Huang S C, Chen Y F, et al. Efficient high-peak-power AlGaInAs eye-safe wavelength disk laser with optical in-well pumping [J]. Optics Express, 2009, **17**(14): 11409 - 11414.

[4] Zhang Y G, Gu Y. Gas source MBE grown wavelength extending InGaAs photodetectors[M]. Ed: Gian-Franco D B,

(下转第 398 页)

468－470.
[3]Knapp H, Meister T F, Liebl W, *et al.* 168 GHz dynamic frequency divider in SiGe:C bipolar technology [J]. 2009 *IEEE Bipolar/BiCMOS Circuits and Technology Meeting - BCTM*, 2009: 190－193|209.
[4]Su Y, Jin Z, Cheng W, *et al.* An InGaAs/InP 40 GHz CML static frequency divider[J]. *Journal of Semiconductors*, 2011: 035008 (035004 pp.).
[5]Jin Z, Su Y B, Cheng W, *et al.* High-breakdown-voltage submicron InGaAs/InP double heterojunction bipolar transistor with f(t) = 170 GHz and f(max) = 253GHz [J]. *Chinese Physics Letters*, 2008, **25**(7): 2686－2689.
[6]Jin Z, Su Y B, Cheng W, *et al.* High-speed InGaAs/InP double heterostructure bipolar transistor with high breakdown voltage[J]. *Chinese Physics Letters*, 2008, **25**(7): 2683－2685.
[7]Jin Z, Su Y B, Cheng W, *et al.* High current multi-finger InGaAs/InP double heterojunction bipolar transistor with the maximum oscillation frequency 253 GHz [J]. *Chinese Physics Letters*, 2008, **25**(8): 3075－3078.
[8]Ge J, Jin Z, Su Y B, *et al.* A physical-model of small-signal InP-based double heterojunction bipolar transistors and its parameter extraction technique [J]. *Acta Physica Sinica*, 2009, **58**(12): 8584－8590.
[9]Ge J, Jin Z, Su Y B, *et al.* A Physics-Based Charge-Control Model for InP DHBT Including Current-Blocking Effect [J]. *Chinese Physics Letters*, 2009, **26**(7).
[10]Leijun X, Zhigong W, Qin L, *et al.* Modelling and Design of a Wideband Marchand Balun [J]. 2010 *Asia-Pacific Symposium on Electromagnetic Compatibility* (*APEMC* 2010), 2010: 1374－1377.
[11]Sun J S, Chen G Y, Huang S Y, *et al.* The wideband marchand balun transition design [J]. 2006 7*th International Symposium on Antennas, Propagation and EM Theory*, *Vols* 1 *and* 2, *Proceedings*, 2006: 796－799.
[12]O. Kappeler, A. Leuther, W. Benz, *et al.* 108 GHz dynamic frequency divider in 100 nm metamorphic enhancement HEMT technology [J] *Electron. Lett.*, 2003, 39: 989－990.
[13]Satoshi Tsunashima, Hiroki Nakajima, Eiichi Sano, *et al.* 90-GHz operation of a novel dynamic frequency divider using InP/InGaAs HBTs [J]. 2002 *Indium Phosphide and Related Materials conference*, 2002:43－46.
[14] *Satoshi Tsunashima*, *Koichi Murata*, *Minoru Ida*, et al. *A 150-GHz dynamic frequency divider using InPllnGaAs DHBTs* [*J*]. IEEE GaAs Digest, 2003:284－287.

(上接第388页)

Advances in Photodiodes, Croatia: InTech, 2011, 349－376.
[5]Selmic S R, Chou T M, Sih J P, et al. Design and characterization of 1.3 μm AlGaInAs-InP multiple-quantum-well lasers [J]. IEEE Journal of Selected Topics in Quantum Electronics, 2001, **7**(2): 340－349.
[6]Cheng J, Shieh C L, Huang X, et al. Efficient CW lasing and high-speed Modulation of 1.3 μm AlGaInAs VCSELs with good high temperature lasing performance [J]. IEEE Photonics Technology Letters, 2005, **17**(1): 7－9.
[7]Watanabe I, Sugou S, Ishikawa H, et al. High-speed and low-dark-current flip-chip InAlAs/InAlGaAs quaternary well superlattice APDs with 120 GHz gain-bandwidth product [J]. IEEE Photonics Technology Letters, 1993, **5**(6): 675－677.
[8] Goldstein L, Praseuth J P, Joncour M C, et al. MBE growth of $Al_xGayIn1-_x-yAs$ for a DHBT structure [J]. Journal of Crystal Growth, 1987, **81**(1-4): 396－399.
[9]Liu W C, Wang, W C, Pan H J, et al. Multiple-route and multiple-state current-voltage characteristics of an InP/AlInGaAs switch for multiple-valued logic applications [J]. IEEE Transactions on Electron Devices, 2000, **47**(8): 1553－1559.
[10]Wu C S, Chan Y J, Shien J L, et al. In0.52(Al0.9Ga0.1)0.48As/In0.53Ga0.47As HEMT with improved device reliability [J]. Electronics Letters, 1995, **31**(13): 1105－1106.
[11]Whelan C S, Hoke W F, McTaggart RA, et al. Low noise In0.32(AlGa)0.68As/In0.43Ga0.57As metamorphic HEMT on GaAs substrate with 850 mW/mm2 output power density [J]. IEEE Electron Device Letters, 2000, **21**(1): 5－8.
[12]Chua S J, Ramam A. Photoluminescence observations in band-gap tailored InGaAlAs epilayers lattice matched to InP substrate [J]. Journal of Applied Physics, 1996, **80**(8): 4604－4608.